Short-range order in some alloys of the Ge–As–Te semiconducting glassy system by X-ray diffraction

R. A. LIGERO, J. VÁZQUEZ, P. VILLARES, R. JIMÉNEZ-GARAY
Departamento de Física Fundamental, Facultad de Ciencias, Universidad de Cádiz, Apartado 40, Puerto Real, Cádiz, Spain

A study of short-range order in amorphous semiconducting alloys of the Ge–As–Te system has been carried out by X-ray diffraction. The different hypotheses on germanium coordination have been taken into account, following the different criteria cited in the literature for binary Ge–Te alloys. The result of this study shows the possibility of structural units based on tetra- or tricoordinated germanium atoms, which bonded together give way to short-range order in these alloys. It has also been found that, for these alloys, germanium dicoordination is not compatible with the data obtained experimentally.

1. Introduction
There has been considerable progress in glass science in the last few years. Reversible electrical switching and lock-on phenomena have been observed in several amorphous chalcogenide semiconductors [1–3]. Amorphous alloys of the Ge–As–Te system exhibit these electrical properties [4–8]. The features of these properties depend strongly on structure.

Chalcogenide glasses with polivalent elements exhibit properties which are the result of the formation of tridimensional structural units. These polivalent atoms, which stabilize the chalcogenide structures, are preferably arsenic and germanium, which form space units with the chalcogen elements, break their characteristic complex structural formations and contribute to the establishments of more homogeneous structures for the glassy alloys belonging to this type of system, a fact which explains some of the properties mentioned.

Analysis of short-range structure in alloys $Ge_{0.05}As_{0.20}Te_{0.75}$, $Ge_{0.10}As_{0.20}Te_{0.70}$ and $Ge_{0.14}As_{0.43}Te_{0.43}$ has been carried out, bearing in mind all the above-mentioned reasons, from the radial distribution function (RDF) of each of these alloys, obtained by X-ray diffraction. The experimental values of the area under the first peak of the RDF have been compared to those obtained theoretically for the values of this magnitude [9, 10], as a germanium coordination function and bearing in mind that functions $R_{ij}(s) = f_i(s)f_j(s)/[\Sigma_i x_i f_i(s)]^2$, depend on the scattering angle [11] and cannot always be approximated by constant value $Z_iZ_j/(\Sigma_i x_iZ_i)^2$.

2. Experimental details
The bulk samples were obtained using the melt–quench method [12]. Adequate proportions of the elements germanium, arsenic and tellurium, 99.999% nominal purity were weighed to obtain 7 g samples. The mixtures were put into vacuum-sealed quartz ampoules in an inert atmosphere of helium. The ampoules were placed into a rotary oven at a temperature of 1000° C for one day, and were quenched in an ice–water bath.

The ingots were removed from the quartz ampoules by introducing these into a corrosive mixture of hydrofluoride acid and hydrogen peroxide.

The amorphous character of the samples was tested by X-ray diffraction. Densities were measured using a pycnometric method, at room temperature; the results obtained are shown in Table I.

The intensities diffracted by each of the samples were measured in a Siemens D500 diffractometer, using Bragg–Brentano geometry by reflection, equipped with a bent graphite monochromator, scintillation counter and standard electronics. The radiation used was $MoK_\alpha (\lambda = 0.071\,069\,nm)$.

For each of the samples, four scans were done in the $5° \leqslant 2\theta \leqslant 110°$ interval, using an adequate opening so that the radiated sample surface was always the same. In order to keep the procedure error constant during the whole scan, the time periods corresponding to a fixed number of counts were measured ($n = 4000$).

3. Radial distribution function
The intensities observed were corrected in background, polarization and multiple scattering [13]. Compton correction was also carried out, taking into account the efficacy of the monochromator, following the procedure described by Shevchik [14]. Thus corrected, the intensities were normalized to electron units (e.u.) using the high-angle method [13], by adjusting the experimental function to the independent scattering function of the alloy, using a square least method

$$I_{exp}(e.u.) = K_1 I_{a.u.}\, e^{-K_2 s^2} \tag{1}$$

$I_{a.u.}$ being the corrected experimental intensities, s ($= 4\pi \sin \theta/\lambda$) the scattering vector module, and K_1
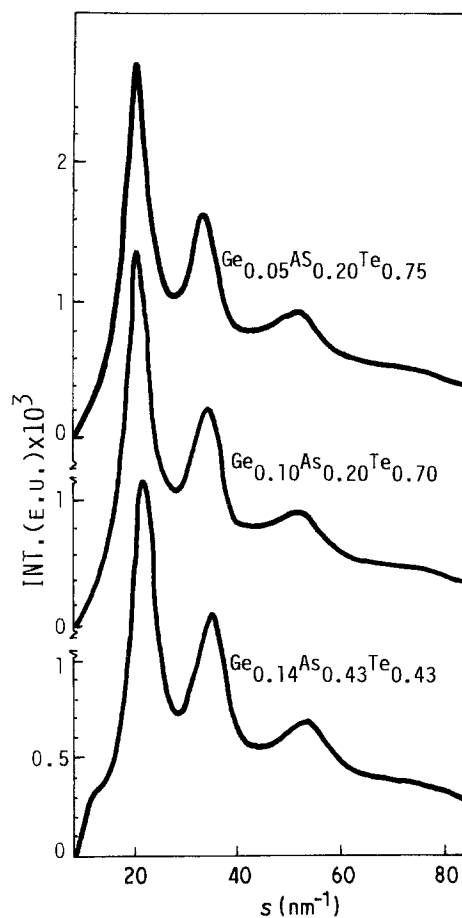
Figure 1 Intensities in electron units.

in which $\varrho(r)$ is local atomic density, which is affected by the Fourier transformation of the products $R_{ij}(s) = f_i(s)f_j(s)/|\Sigma_i x_i f_i(s)|^2$ and ϱ_0 is average experimental atomic density of the material, expressed in atoms/$\mathring{A}^3$.

The spurious oscillations, which appear in RDF before the first significant maximum due to lack of experimental data for high values of s, force us to extend the interference function to $s_{max} = 300\,\mathrm{nm}^{-1}$ for which function $F(s)$ tends to zero. The extension was done using the method described by d'Anjou and Sanz [15], based on that proposed by Shevchik [14], according to which, when the values of s are high, the interference function is approximately

$$F_{\text{theoret}}(s) = \frac{C}{r} \sin(sr)\, e^{-\sigma^2 s^2/2} \qquad (5)$$

in which C, r and σ are parameters obtained through least square fitting from initial values C_1, r_1 and σ_1, which represent area, position and half-width of the first RDF peak, deduced from Equation 3 for $s_{max} = 144.8\,\mathrm{nm}^{-1}$, which is the maximum value for which data are obtained with the device used.

The RDFs of the three alloys in the system studied, shown in Fig. 2, were found through Fourier transformation for the extended $F(s)$. Analysis of experimental RDF for each alloy gives the structural information shown in Table I, together with the corresponding experimental densities.

and K_2 the adjustment parameters. Parameter K_1 represents a scale factor, and K_2 is related to the Debye–Waller temperature factor. In Fig. 1 the intensities for the alloys studied are shown.

From the intensities normalized to e.u., the reduced intensities, $i(s)$ are obtained thus:

$$i(s) = \frac{I_{e.u.}(s) - \sum_i x_i f_i^2(s)}{\left[\sum_i x_i f_i(s)\right]^2} \qquad (2)$$

x_i and $f_i(s)$ being atomic fraction and scattering atomic factor of a type i atom, respectively.

The function $G(r)$, which can be determined by taking Fourier transformation for the interference function, $F(s) = si(s)$, is expressed by the relation

$$G(r) = \frac{2}{\pi} \int_0^{s_{max}} F(s) \sin sr \, ds \qquad (3)$$

which gives the radial distribution function (RDF):

$$4\pi r^2 \varrho(r) = 4\pi r^2 \varrho_0 + rG(r) \qquad (4)$$

4. RDF analysis

The definition interval of the first peak of the RDF for each of the alloys, which corresponds to the first coordination sphere, is such that in all cases, all types of bonds are possible between the different elements of the Ge–As–Te system (Ge = 1, As = 2, Te = 3), as may be observed by comparing each interval to the bond lengths cited in the literature, which are summarized in Table II.

Analysis of experimental RDF shows a fact which is very interesting when carrying out a model of the short-range order of a glassy solid: the area under the first peak, represents the number of atoms which, on average, surround any given one taken as a reference, i.e. the average coordination number for the material.

Bearing in mind the physical significance of this area, and that the products $R_{ij}(s)$ are functions of the scattering angle, Vázquez and Sanz [11], following the method described by Warren [13], have concluded that the area under the first RDF peak is related to certain structural parameters, relative coordination

TABLE I RDF characteristics

	$Ge_{0.05}As_{0.20}Te_{0.75}$		$Ge_{0.10}As_{0.20}Te_{0.70}$		$Ge_{0.14}As_{0.43}Te_{0.43}$	
Maximum	1	2	1	2	1	2
Position (nm)	0.270	0.410	0.270	0.405	0.260	0.395
Limits (nm)	0.235–0.305		0.240–0.310		0.225–0.305	
Averaged angle (deg.)	98.8		97.18		98.86	
Area (at.)	2.05	6.89	2.10	6.90	2.42	6.97
Error	±0.1	±0.2	±0.1	±0.2	±0.1	±0.2
Density (g cm^{-3})	5.72		5.66		5.51	

Figure 2 Radial distribution functions.
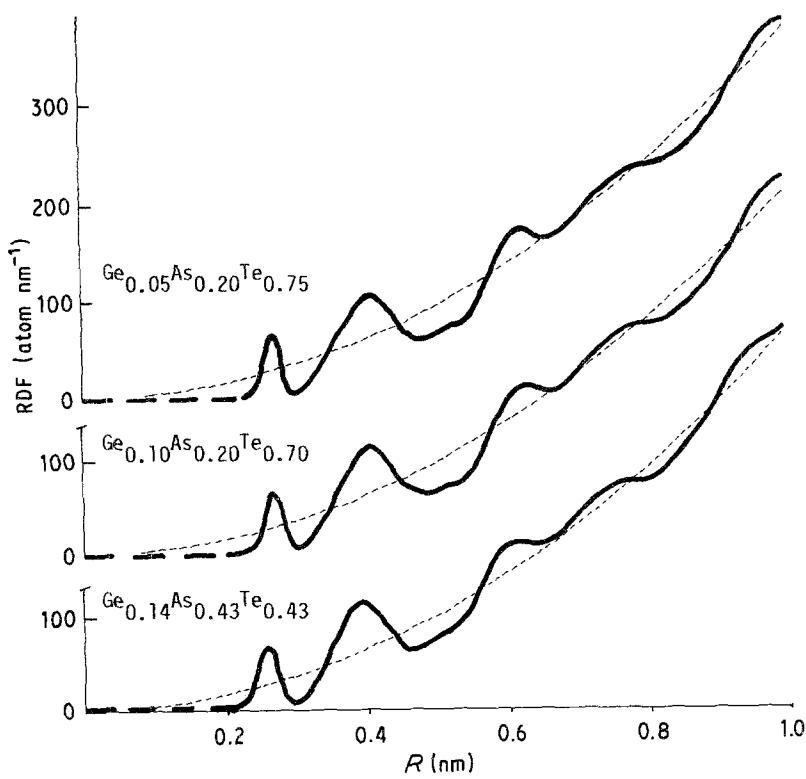
numbers, n_{ij}, by the expression

$$\text{Area} = \frac{2}{\pi} \sum_i \sum_j x_i \frac{n_{ij}}{r_{ij}} \int_a^b r P_{ij}(r) \, dr \qquad (6)$$

r_{ij} being the average distance between a type i and a type j atom, a and b the limits of the first RDF peak and $P_{ij}(r)$ a function defined by

$$P_{ij}(r) = \frac{1}{2} \int_0^{s_m} \frac{f_i(s)f_j(s)}{\left[\sum_i x_i f_i(s)\right]^2} \cos s(r - r_{ij}) \, ds \qquad (7)$$

s_m being the upper measurement limit.

The structural information obtained by analysis of experimental RDF, together with certain physical–chemical properties of the alloys and their elements, give way to hypotheses on the local order of glassy alloys. These hypotheses, reflected in the relative coordination numbers, n_{ij}, and consequently in the number of chemical bonds between the different pairs of elements in a material, have allowed Vázquez et al. [10] to deduce, from Equation 6, the following relationship:

$$\text{Area} = \frac{1}{50\pi} \left[\left(h + \beta A_{22} - \delta \sum_{i,j \neq 1} A_{ij} \right) N \right.$$

$$+ \alpha A_{22} + \gamma \sum_{i,j \neq 1} A_{ij}$$

$$\left. + P \left(\sum_{i=j \neq 1} A_{ij} - \sum_{\substack{i,j \neq 1 \\ i \neq j}} A_{ij} \right) a_{ij} \right] \qquad (8)$$

where h, α, β, γ and δ are parameters characteristic of each alloy, N the coordination attributed to a given element of the alloy, P a parameter whose value is 2 when in variable a_{ij}, $i = j$, and -1 if $i \neq j$, and A_{ij} is determined by

$$A_{ij} = \frac{1}{r_{ij}} \int_a^b r P_{ij}(r) \, dr \qquad (9)$$

In this work, in order to evaluate the A_{ij} parameters, the $R_{ij}(s)$ functions have been adjusted to the corresponding regression straight lines, and the values shown in Table III have been calculated by the method described by Vázquez and Sanz [11]. The following results have been obtained for the specific characteristics of each alloy:

$h = 3.3202 \quad \alpha = -101.58 \quad \beta = 2.89$

$\gamma = 165.79 \quad \delta = 3.95 \quad \text{for } Ge_5$

$h = 5.5782 \quad \alpha = -102.18 \quad \beta = 5.04$

$\gamma = 170.09 \quad \delta = 7.02 \quad \text{for } Ge_{10}$

$h = 12.6039 \quad \alpha = 43 \quad \beta = 0$

$\gamma = 114 \quad \delta = 7 \quad \text{for } Ge_{14}$

Equation 8, which gives the area under the first peak as a function of coordination, N, and of the number of bonds, a_{ij}, of the pair of elements i, j, has been used to evaluate this area in each of the studied

TABLE II Bond lengths

Pair	r_{ij} (nm)	Ref.
Ge–Ge	0.251	[16]
Ge–As	0.244	[16]
Ge–Te	0.258	[17]
As–As	0.257	[8]
As–Te	0.258	[8]
Te–Te	0.260	[18]

TABLE III A_{ij} parameters

Pair	A_{ij}		
	$Ge_{0.05}As_{0.20}Te_{0.75}$	$Ge_{0.10}As_{0.20}Te_{0.70}$	$Ge_{0.14}As_{0.43}Te_{0.43}$
1–1	0.6959	0.5911	0.9376
1–2	0.7017	0.4840	0.9488
1–3	1.1604	1.1916	1.5577
2–2	0.7423	0.7144	0.9975
2–3	1.2002	1.1855	1.6123
3–3	1.9377	2.0357	2.6009

TABLE IV Theoretical results obtained for the different coordination hypotheses of the germanium atom

Alloy*	Theoretical area	Coordination numbers n_{ij}, $i, j \neq 1$	N	Variation intervals for parameter a_{33}		Intersection of intervals
				Defined by the n_{ij} parameters	Defined by limits of error of the experimental area	
A	$2.0535 - 0.0255N$ $+ 0.0036a_{33}$	$n_{22} = -5.0789 + 0.2822N + 0.1a_{33}$ $n_{23} = 8.2895 - 0.3849N - 0.1a_{33}$	4	$39.50 \leqslant a_{33} \leqslant 67.50$	$0 \leqslant a_{33} \leqslant 55.14$	$39.50 \leqslant a_{33} \leqslant 55.14$
			3	$42.32 \leqslant a_{33} \leqslant 71.35$	$0 \leqslant a_{33} \leqslant 48.06$	$42.32 \leqslant a_{33} \leqslant 48.06$
			2	$45.14 \leqslant a_{33} \leqslant 75.20$	$0 \leqslant a_{33} \leqslant 40.97$	–
B	$2.1027 - 0.0475N$ $+ 0.0048a_{33}$	$n_{22} = -5.1088 + 0.4817N + 0.1a_{33}$ $n_{23} = 8.5044 - 0.6706N - 0.1a_{33}$	4	$31.82 \leqslant a_{33} \leqslant 58.22$	$18.19 \leqslant a_{33} \leqslant 59.85$	$31.82 \leqslant a_{33} \leqslant 58.22$
			3	$36.64 \leqslant a_{33} \leqslant 64.93$	$8.29 \leqslant a_{33} \leqslant 49.96$	$36.64 \leqslant a_{33} \leqslant 49.96$
			2	$41.45 \leqslant a_{33} \leqslant 71.63$	$0 \leqslant a_{33} \leqslant 40.06$	–
C	$2.6133 - 0.0635N$ $+ 0.0048a_{33}$	$n_{22} = 1 + 0.0465a_{33}$ $n_{23} = 2.6512 - 0.3028N - 0.0465a_{33}$	4	$0 \leqslant a_{33} \leqslant 30.97$	$0 \leqslant a_{33} \leqslant 33.48$	$0 \leqslant a_{33} \leqslant 30.97$
			3	$0 \leqslant a_{33} \leqslant 37.48$	$0 \leqslant a_{33} \leqslant 20.25$	$0 \leqslant a_{33} \leqslant 20.25$
			2	$0 \leqslant a_{33} \leqslant 43.99$	$0 \leqslant a_{33} \leqslant 7.02$	$0 \leqslant a_{33} \leqslant 7.02$

*A $= Ge_{0.05}As_{0.20}Te_{0.75}$, B $= Ge_{0.10}As_{0.20}Te_{0.70}$, C $= Ge_{0.14}As_{0.43}Te_{0.43}$.

alloys in the Ge–As–Te system, expressing it as a function of the number of Te–Te bonds, a_{33}.

Bearing in mind the models based on the coordination scheme proposed by Hilton et al. [19], and following the coordination hypotheses postulated by Betts et al. [20] for binary alloys of the Ge–Te system, the present work analyses the possibility of proposing structural units for the configuration of short-range order in the alloys under study, in tetra-, tri- and dicoordinated germanium, respectively.

This analysis consists, on the one hand, of determining the theoretic area under the first RDF peak for each alloy and each of the coordination hypotheses for germanium and comparing it to the corresponding experimental area. This comparison defines the a_{33} variation intervals for each alloy.

On the other hand, as the area is a function of the relative coordination numbers which, in turn, depend on the coordination number, N, of a certain element, germanium, in the alloy [9], it is necessary to determine the variation field for a_{33}, due to the restrictions imposed by the intrinsically positive nature of n_{ij}.

When proposing local order models, the intersection of both intervals give us the possible variability field for parameter a_{33}.

When expressing the area as a function of the number of Te–Te bonds, the n_{ij} which enclose a_{33} are given by [9]

$$n_{22} = \frac{\alpha + [(100 + a_2' + a_3')/100]\beta N + 2a_{33}}{a_2'}$$

(10a)

$$n_{23} = \frac{\gamma - [(100 + a_2' + a_3')/100]\delta N - 2a_{33}}{a_2'}$$

(10b)

The area expressions in Table IV are obtained for each alloy through Equation 8, using the A_{ij} in Table III and the corresponding characteristic parameters; together with the corresponding experimental area (Table I), within a margin of error of ± 0.1 atoms, they determine the variation intervals of a_{33} (always a positive magnitude) for each coordination hypothesis, which are shown in Table IV.

On the other hand, Equations 10a and 10b give the expressions of n_{22} and n_{23}, which establish the new limits for magnitude a_{33}, shown in Table IV together with their intersections with the corresponding intervals for the margin of error of the experimental area.

As an illustration of the theoretical calculations carried out, Fig. 3 shows the theoretically obtained areas plotted against the number of Te–Te bonds, according to the tetra- and tricoordinated germanium hypotheses, for alloy $Ge_{0.10}As_{0.20}Te_{0.70}$. This figure shows the intervals at which the areas are simultaneously compatible with the experimental area and the corresponding coordination numbers.

Analysis of the intervals intersection leads to the conclusion that the dicoordinated germanium hypothesis is incompatible with the structural information obtained from experimental data for the three alloys studied, a fact which is in accordance with the conclusions reached by Betts et al. [20] for Ge–Te binary alloys. In the first two alloys, this incompatibility shows itself immediately by the fact that there exists no number of Te–Te bonds which, keeping coordination
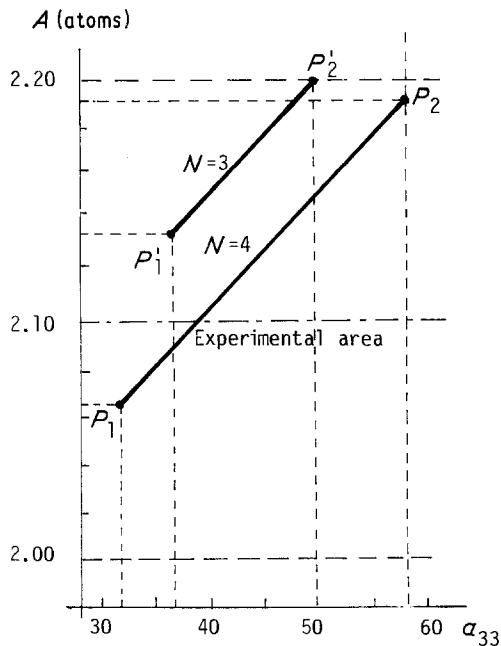

Figure 3 Areas of first peak plotted against number of Te–Te bonds for $Ge_{0.10}As_{0.20}Te_{0.70}$ alloy.

numbers n_{22} and n_{23} positive, simultaneously originate a theoretical area inside the margin of error of the experimental area. As to the third alloy, dicoordinated germanium is not acceptable either because, although the study shows the possibility of considering $N = 2$ for this element, the maximum number of Te–Te bonds per 100 atoms of material would be 7, too small a value considering the high tellurium concentration in the sample and the strong chain-forming tendency of this element, as in the case of selenium [21, 22].

5. Conclusions

According to the radial distribution functions obtained for each of the alloys studied in the Ge–As–Te glassy system, from X-ray diffraction data and the analysis of different germanium-coordination hypotheses, it has been found that tri- and tetra-coordination for this element are possible in these samples, but the dicoordinated germanium hypothesis is not compatible with experimentally obtained data.

The structural configuration most in agreement with the experimental data for the three alloys could be a network of tetrahedral units centred on germanium atoms and coexisting with others in which this element occupies a vertex of triangular pyramids, the rest of them being taken by any one of the different atoms that constitute the material.

References

1. S. R. OVSHINSKY, *Phys. Rev. Lett.* **21** (1968) 1450.
2. R. UTTECHT, H. STEVENSON, C. H. SIE, J. D. GRIENER and K. S. RAGHAVEN, *J. Non-Cryst. Solids* **2** (1970) 358.
3. E. MÁRQUEZ, P. VILLARES and R. JIMÉNEZ-GARAY, *Mater. Lett.* **4** (1986) 52.
4. *Idem, J. Non-Cryst. Solids* **74** (1985) 195.
5. K. TANAKA, Y. OKADA, M. SUGI, S. IIZIMA and M. KIKUCHI, *ibid.* **12** (1973) 100.
6. M. HARO, E. MÁRQUEZ, L. ESQUIVIAS and R. JIMÉNEZ-GARAY, *ibid.* **81** (1986) 255.
7. E. MÁRQUEZ, P. VILLARES and R. JIMÉNEZ-GARAY, *Mater. Lett.* **3** (1985) 503.
8. J. VÁZQUEZ, E. MÁRQUEZ, P. VILLARES and R. JIMÉNEZ-GARAY, *ibid.* **4** (1986) 360.
9. J. VÁZQUEZ, L. ESQUIVIAS, P. VILLARES and R. JIMÉNEZ-GARAY, *Ann. Fis. B* **81** (1985) 223.
10. J. VÁZQUEZ, P. VILLARES and R. JIMÉNEZ-GARAY, *Mater. Lett.* **4** (1986) 485.
11. J. VÁZQUEZ and F. SANZ, *Ann. Fis. B* **80** (1984) 31.
12. J. VÁZQUEZ, P. VILLARES and R. JIMÉNEZ-GARAY, *J. Non-Cryst. Solids* **86** (1986) 251.
13. B. E. WARREN, "X-ray diffraction" (Addison-Wesley, Reading, 1969).
14. N. J. SHEVCHIK, PhD thesis, Harvard University (1972).
15. A. d'ANJOU and F. SANZ, *J. Non-Cryst. Solids* **28** (1978) 319.
16. N. de la ROSA-FOX, L. ESQUIVIAS, P. VILLARES and R. JIMÉNEZ-GARAY, *Phys. Rev. B* **33** (1986) 4094.
17. L. PAULING, "Uniones Químicas" (Kapelusz, Buenos Aires, 1969).
18. J. VÁZQUEZ, P. VILLARES and R. JIMÉNEZ-GARAY, *Mater. Lett.* **4** (1986) 171.
19. A. R. HILTON, C. E. JONES, R. D. DOBROTT, H. M. KLEIN, A. M. BRYANT and T. D. GEORGE, *Phys. Chem. Glasses* **4** (1966) 116.
20. F. BETTS, A. BIENENSTOCK, D. T. KEATING and J. P. de NEUFVILLE, *J. Non-Cryst. Solids* **7** (1972) 417.
21. G. TOURAND, B. CABANE and M. BREUIL, *ibid.* **8-10** (1972) 676.
22. B. W. CORB, W. D. WEI and B. L. AVERBACH, *ibid.* **53** (1982) 29.